Engineered human Diamond-Blackfan anemia disease model confirms therapeutic effects of clinically applicable lentiviral vector at single-cell resolution

Yang Liu,[1,2*] Ludwig Schmiderer,[1*] Martin Hjort,[3,4,5] Stefan Lang,[6] Tyra Bremborg,[1] Anna Rydström,[1] Axel Schambach,[7,8] Jonas Larsson[1] and Stefan Karlsson[1]

[1]Division of Molecular Medicine and Gene Therapy, Lund Stem Cell Center, Lund University, Lund, Sweden; [2]Department of Medicine, Huddinge, Karolinska Institutet, Stockholm, Sweden; [3]Chemical Biology and Therapeutics, Department of Experimental Medical Science, Lund University, Lund, Sweden; [4]Navan Technologies, MBC Biolabs, San Carlos, CA, USA; [5]NanoLund, Lund University, Lund, Sweden; [6]Division of Molecular Hematology and Stem Cell Center, Lund University, Lund, Sweden; [7]Institute of Experimental Hematology, Hannover Medical School, Hannover, Germany and [8]Division of Hematology/Oncology, Boston Children's Hospital, Harvard Medical School, Boston, MA, USA

**YL and LS contributed equally as first authors.*

Correspondence: Yang Liu
yang.liu@med.lu.se

Stefan Karlsson
stefan.karlsson@med.lu.se

Received: September 8, 2022.
Accepted: May 11, 2023.
Early view: May 18, 2023.

https://doi.org/10.3324/haematol.2022.282068

Abstract

Diamond-Blackfan anemia is a rare genetic bone marrow failure disorder which is usually caused by mutations in ribosomal protein genes. In the present study, we generated a traceable *RPS19*-deficient cell model using CRISPR-Cas9 and homology-directed repair to investigate the therapeutic effects of a clinically applicable lentiviral vector at single-cell resolution. We developed a gentle nanostraw delivery platform to edit the *RPS19* gene in primary human cord blood-derived CD34$^+$ hematopoietic stem and progenitor cells. The edited cells showed expected impaired erythroid differentiation phenotype, and a specific erythroid progenitor with abnormal cell cycle status accompanied by enrichment of TNFα/NF-κB and p53 signaling pathways was identified by single-cell RNA sequencing analysis. The therapeutic vector could rescue the abnormal erythropoiesis by activating cell cycle-related signaling pathways and promoted red blood cell production. Overall, these results establish nanostraws as a gentle option for CRISPR-Cas9-based gene editing in sensitive primary hematopoietic stem and progenitor cells, and provide support for future clinical investigations of the lentiviral gene therapy strategy.

Introduction

Diamond-Blackfan anemia (DBA) is a rare genetic bone marrow failure disorder characterized by anemia and is associated with physical malformations and a predisposition to cancer. Around 75% of DBA cases are related to a heterozygous allelic variation in ribosomal protein genes of either small or large ribosomal subunit.[1] The most frequently affected gene is ribosomal protein S19 (RPS19), which accounts for approximately 25% of the cases that occur in 6 out of 1 million live births.[2] The defect has been defined functionally by a reduced ability to generate erythroid burst-forming unit (BFU-E) and erythroid colony-forming unit (CFU-E) colonies, and are associated with aberrant ribosome biogenesis and activation of p53-dependent apoptotic pathways.[1,3,4] However, despite significant progress in understanding the molecular basis of DBA pathophysiology, up to now, there is no curable treatment for patients except allogeneic bone marrow transplantation.[1,2]

Our group recently developed a self-inactivating lentiviral vector containing a codon-optimized *RPS19* cDNA driven by the clinically applicable promoter, shortened version of human elongation factor 1α (EFS), and demonstrated the therapeutic effects in *RPS19*-deficient DBA mice.[5] Due to the very limited availability of patient samples, creating a human cell model that faithfully mimics the naturally occurring loss of *RPS19* would be critical for the development of a gene therapy approach that can eventually be used to treat patients. To achieve this, we aimed to generate a *RPS19* haploinsufficient cell model using CRISPR-Cas9 (Cas9) and an adeno-associated virus (AAV)-based HDR template carrying a traceable marker gene via homologous recombination that can be used to label and identify successfully edited cells by their marker gene expression. Initially, we de-

livered Cas9 editing cargo with electroporation, but found it difficult to recover sufficient numbers of viable edited cells. This is likely due to a combination of several factors. First, since homozygous loss of *RPS19* is lethal, any biallelic knockout (KO) cells are not expected to be viable.[2,6-8] Secondly, heterozygous *RPS19* KO cells are expected to be viable, but highly sensitive to stress, since monoallelic loss of *RPS19* generates nucleolar stress, p53 stabilization and activation of its targets.[1] Last but not least, both electroporation and Cas9 activity have been shown to impair the function and viability of treated hematopoietic stem and progenitor cells (HSPC).[9,10] The combined stress of these factors makes it challenging to generate an ideal *RPS19*-deficient CD34$^+$ HSPC model.

Novel non-viral transfection methodologies such as nanostraws have been shown to be a gentle and non-toxic alternative to electroporation.[11-13] Nanostraws are hollow alumina nanotubes that can be used to inject mRNA and other biomolecules directly into the cytoplasm via the application of a gentle, pulsed electric field.[11] Until now, however, they have only been used to successfully deliver smaller mRNA (e.g., gene fluorescent protein, GFP) to human HSPC. Efficient nanostraw-mediated Cas9 delivery to primary cells has so far not been demonstrated, even though this would be a major advancement for the generation of desired cell models in situations where the number of available cells is limited.

In the present study, we demonstrate nanostraw-mediated Cas9 mRNA delivery that enables gentle gene editing in human CD34$^+$ HSPC. Using this approach, we successfully generated a traceable *RPS19*-deficient cell model, and confirm the therapeutic effect of the therapeutic vector with erythroid differentiation assays and single-cell transcriptomics.

Methods

Primary human samples, isolation and transduction of hematopoietic stem and progenitor cells

Human cord blood samples were obtained from the maternity wards of Helsingborg General Hospital and Skåne University Hospital in Lund and Malmö, Sweden, after informed, written consent according to guidelines approved by the regional ethical committee. Mononuclear cells were separated through density-gradient centrifugation, as described previously.[5] Cells were cultured in serum-free expansion medium, supplemented with stem cell factor, thrombopoietin, and FLT3-ligand at 100 ng/mL (all from Stem Cell Technologies). Transduction of the therapeutic lentiviral vector was performed at a multiplicity of infection (MOI) of 5, according to the published protocol.[5]

Other experimental methods

Descriptions of other methods used in the study are provided in the *Online Supplementary Appendix*.

Results

Delivery of Cas9 and *RPS19*-targeting sgRNA with electroporation leads to loss of cell viability

The primary aim of the study was to create a traceable *RPS19*-deficient cell model using Cas9 via homologous recombination in cord blood-derived human CD34$^+$ HSPC.[14] To this end, we selected a sgRNA with high editing efficiency and which causes an obviously impaired erythroid differention block phenotype (*Online Supplementary Figure S1A, B*). To make the edited cell traceable, we designed a complementary adeno-associated virus (AAV)-based homology-directed repair (HDR) template that allows GFP expression driven by PGK promoter (Figure 1A) (see Methods). With this system, cells with the expected *RPS19*-deficiency can be distinguished from unedited cells by their GFP expression. Moreover, by taking advantage of the lethal effects of homozygous loss of the *RPS19* gene, the viable GFP$^+$ cells are expected to be carrying heterozygous loss of *RPS19*.[2,6-8] Initially, we used electroporation to deliver Cas9 RNP or mRNA into CD34$^+$ HSPC, followed by AAV transduction at optimized MOI (Figure 1B). Almost no GFP signal can be detected when the MOI is equal or less than 5x10^4 vg/cell on day 4 in the AAV-only treated group (*Online Supplementary Figure S2A-C*). We decided to transduce with AAV at MOI of 5x10^4 vg/cell, which indicates that any GFP signals detected on day 4 or later should be primarily from successful HDR. Considering that the complete loss of *RPS19* causes lethal effects, we included a control condition in which the cell surface marker CD45 was targeted, the KO of which is well tolerated by CD34$^+$ HSPC.[15] The cell viability was measured one day after editing. We found about 26% live cells (7-AAD-Annexin V-) were recovered in the Cas9 RNP *RPS19*-edited group relative to the untreated group (Figure 1C, E) and up to 12% GFP$^+$ cells (Figure 1C, F) on day 1 post electroporation. In the Cas9 RNP *CD45*-edited group, about 35% live cells were recovered relative to the untreated group (*Online Supplementary Figure S3A, C*). On day 4, however, less than 3% live cells in the Cas9 RNP *RPS19*-edited group and 28% live cells in the Cas9 RNP *CD45*-edited group were recovered relative to the untreated group (Figure 1D, E, *Online Supplementary Figure S3B, C*). Importantly, only very few cells carrying the desired edit and template insertion, i.e., being GFP positive, were recovered on day 4 in the *RPS19*-edited group (Figure 1D, F). By counting the total number, only up to 150 live GFP$^+$ cells can be obtained on day 4 from a starting cell number of 2x10^4 CD34$^+$ HSPC, and the low efficiency therefore hinders further downstream analysis. Compared with this, the CD45 KO efficiency is about 63%

in live cells in the Cas9 RNP *CD45*-edited group (*Online Supplementary Figure S3B, D*). This strongly indicates that the loss of *RPS19* has a detrimental effect on the cells, which is possibly exacerbated by the stress from the electroporation. Since the negative effect of electroporation on HSPC function and viability is well documented,[9] we decided to use a milder delivery method that might enable the recovery of higher numbers of successfully edited cells.

Nanostraws enable gentle gene editing with improved cell viability

Arguably the most gentle method of delivering nucleic acids to human HSPC is nanostraws.[10] We previously showed that both the viability and function of $CD34^+$ are fully maintained after nanostraw-mediated delivery of a transiently expressed mRNA (Figure 2A).[10] To investigate if nanostraws could be used for stable gene editing via Cas9 mRNA delivery, we first attempted to KO *CD45* (Figure 2B). As shown in Figure 2C-E, total live cell numbers at a rate of 75% (day 1) and 53% (day 4) relative to completely untreated cells could be recovered upon CD45-targeting using Cas9 mRNA delivery. The efficiency of *CD45* KO can reach up to 23% (Figure 2D, F). We also attempted to deliver Cas9 RNP instead of mRNA, but found that the efficiency was low (approx. 3.5% on average on day 4) (Figure 2D, F), which may be due to the differences in structure and charge between the protein and the GFP-mRNA previously used.[10] Therefore, we decided to use Cas9 mRNA for the following experiments.

We next investigated whether changing the delivery

A

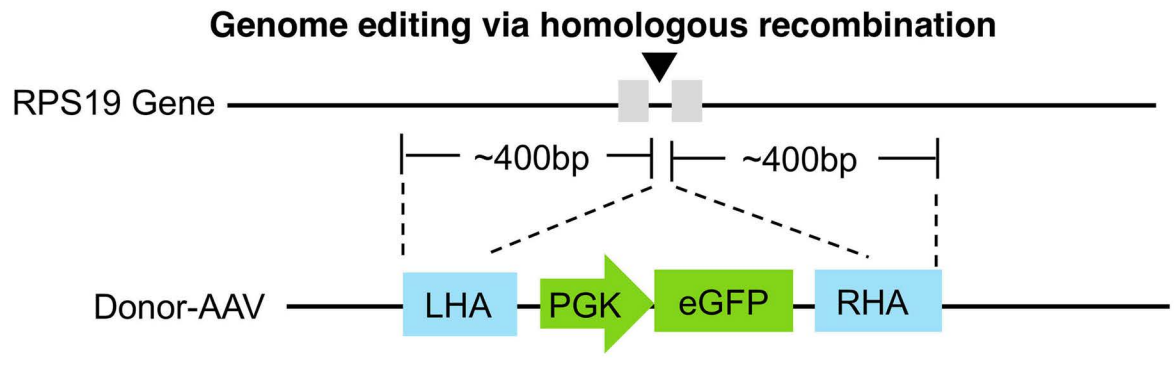

B

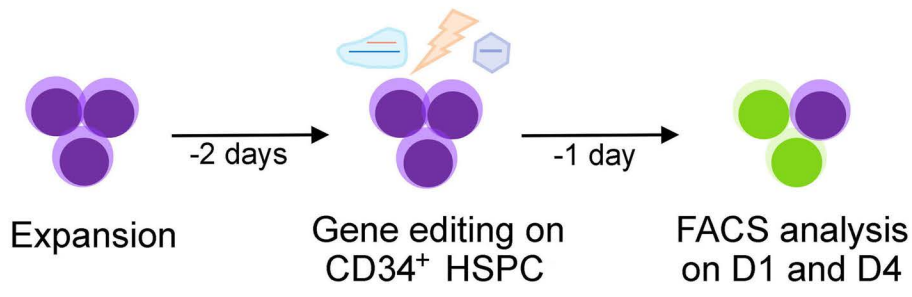

C

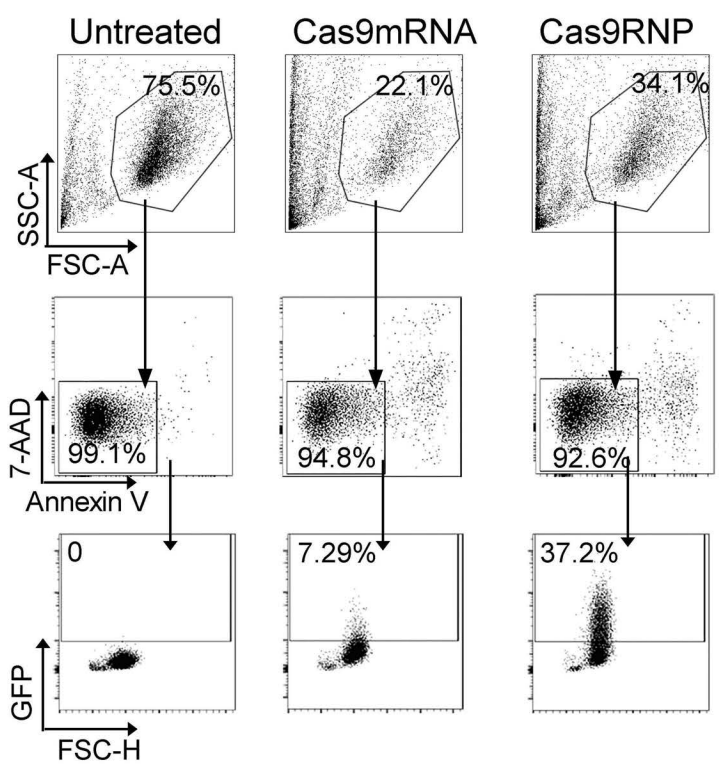

D

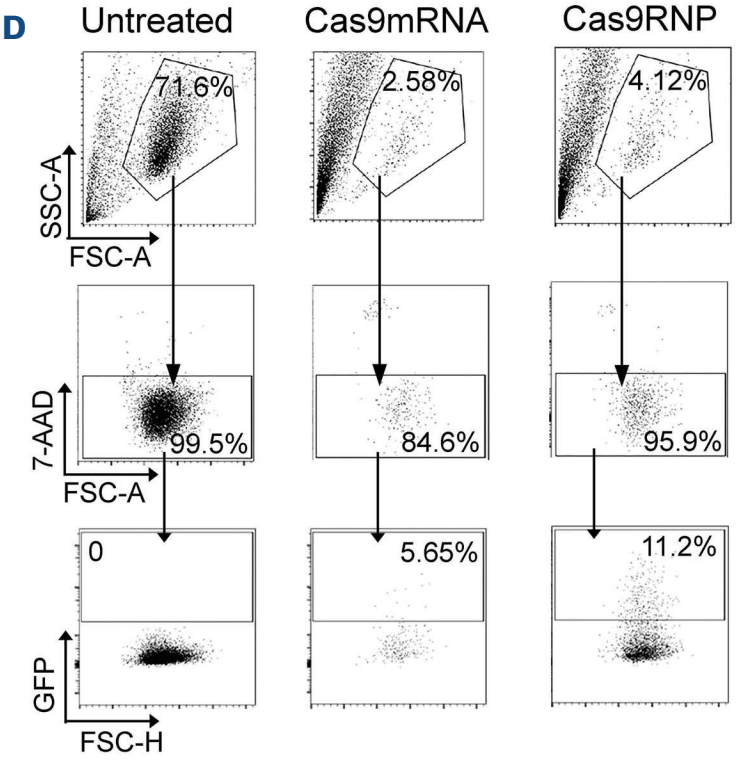

Continued on following page.

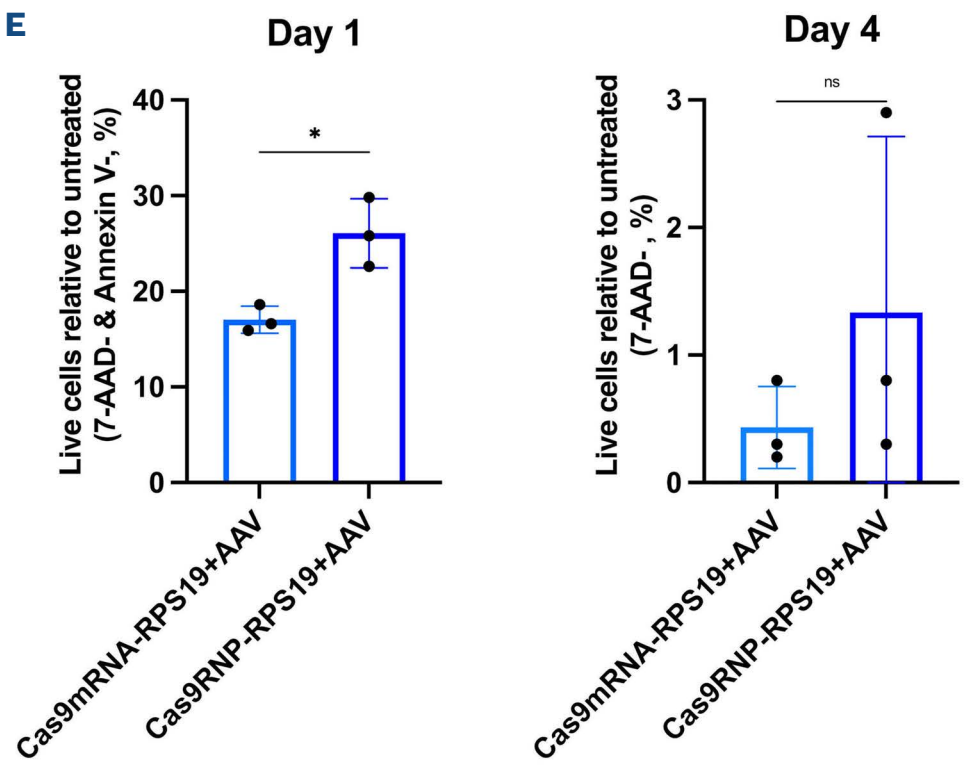

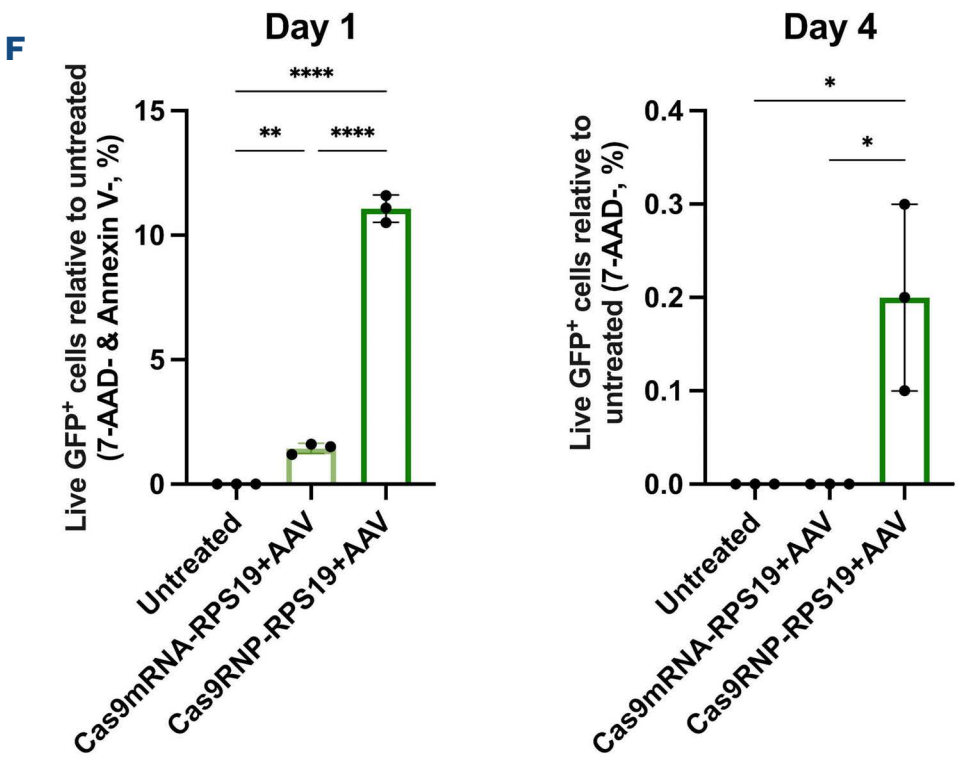

Figure 1. Genome editing via homologous recombination using electroporation leads to strongly decreased cell viability. (A) Schematic overview of RPS19 editing strategy. The RPS19 gene is targeted with Cas9, and gene fluorescent protein (GFP)-encoding adeno-associated virus (AAV) with homology arms flanking the cut site. Successful integration of the homology-directed repair (HDR) template leads to disruption of RPS19 expression, which allows traceable GFP expression. (B) Timeline of experiment. (C and D) Representative FACS plots of cell viability and GFP expression of cells on (C) day 1 and (D) day 4 after electroporation. (E) Percentage of live cell recovery relative to completely untreated cells on days 1 and 4 after electroporation (**P*<0.05 by *t*-test, N=3). (F) Relative percentage of GFP$^+$ cells compared to total recovered live cell numbers of the untreated condition, on days 1 and 4 after electroporation (**P*<0.05, ***P*<0.01, *****P*<0.0001 by one-way ANOVA test, N=3). LHA: left homology arm; RHA: right homology arm; HSPC: hemotopoietic stem and progenitor cells.

method from electroporation to nanostraws could improve the cell viability and recovery of *RPS19*-deficient cells. To this end, we delivered Cas9 mRNA and *RPS19*-targeting sgRNA to CD34$^+$ HSPC with nanostraws and added the AAV HDR-template at the optimized MOI to the cells (Figure 3A). In the *RPS19*-deficient group, we obtained similar numbers of viable cells (7-AAD-Annexin V$^-$) compared to the untreated group on day 1, and 70% 7-AAD$^-$ cells relative to the untreated group on day 4 (Figure 3B, C). This was an enormous improvement over the electroporation results, where less than 3% viable cells compared to the untreated condition could be recovered on day 4. Importantly, we could obtain far more viable GFP$^+$ cells on day 1 (12% on average) and day 4 (1% on average; Figure 3B, D) compared to electroporation (0.2% on average on day 4). On average, nanostraws enabled the recovery of 130-fold more live cells than electroporation, and about 7-fold more GFP$^+$ cells than electroporation when treating the same initial number of cells (*Online Supplementary Figure S4A*). In addition, deep sequencing was performed on edited cells with no HDR template added. The frequency of insertions and deletions (indels) was on average 12% on day 1, but decreased to about 1% on day 4 (*Online Supplementary Figure S4B*). The decrease of the indels likely reflects the lethal effects of homozygous loss of the *RPS19* gene. Consistent with this, we could generate around 1% live GFP$^+$ cells on day 4.

To detect the integration of the HDR template into the RPS19 locus and to assess the differentiation ability of edited cells, we sorted 7-AAD-GFP$^+$ cells from the edited group and 7-AAD$^-$ cells from the mock group. PCR with

primers flanking the homology arms confirmed that the HDR template integrated at the expected site (*Online Supplementary Figure S5A, B*). This was further confirmed by Sanger Sequencing of the PCR product (*Online Supplementary Figure S5C*). To investigate the differentiation ability, a CFU assay was performed. The number of colonies for BFU-E, CFU-G/M/GM, and CFU-GEMM in the edited group was significantly lower than in the mock-treated group (Figure 3E). In particular, GFP can be detected in individual colonies from the edited group (*Online Supplementary Figure S6*). To distinguish mono and bi-allelic integration into the *RPS19* locus of edited cells, single colonies were picked and used to perform digital droplet PCR (ddPCR) (*Online Supplementary Figure S7*). The abundance of the edited allele compared to the alleles of a reference gene (*APOE*, on same chromosome) are in the range of 40-60% in the majority of colonies (85%), which indicated monoallelic integration in the GFP$^+$ cells that successfully formed colonies (Figure 3F). This further confirms the generation of heterozygous *RPS19* loss in our model. In particular, about 15% of all the colonies were found GFP-negative in the edited group on day 14, which may be due to the cytoplasmic non-integrated-AAV that also express GFP when we sorted the cells on day 4, and then gradually became GFP-negative after cell proliferation during culture. Overall, our results demonstrate a successful gentle genome editing strategy for generating *RPS19*-deficient CD34$^+$ HSPC at levels where the edited cells are sufficient for further downstream analysis.

EFS-RPS19 vector rescued impaired erythroid differentiation in *RPS19*-deficient hematopoietic stem and progenitor cells

We next analyzed if the edited cells have the expected erythroid differentiation block phenotype, and whether this disease phenotype can be ameliorated by our therapeutic lentiviral vector, EFS-RPS19. Briefly, *RPS19*-deficient cells (RPS19-D) were generated using nanostraws after 2 days of culture (Figure 4A). A fraction of the RPS19-D cells was transduced with the EFS-RPS19 (LV-RPS19) vector one day later. CD34$^+$ HSPC without treatment (CD34), or Cas9-only treated cells (without sgRNA, named Cas9) were used as control groups. We sorted 7-AAD-GFP$^+$ cells from the RPS19-D group on day 4, and these were cultured in erythroid differentiation medium. On the same day, the expression of endogenous RPS19 and the codon-optimized RPS19 (coRPS19) produced by EFS-RPS19 was measured by RT-qPCR. As expected, expression levels of endogenous RPS19 were strongly reduced in GFP$^+$ cells, which further confirms the successful generation of *RPS19*-deficient CD34$^+$ HSPC (Figure 4B). Interestingly, endogenous *RPS19* expression was significantly reduced in cells transduced with the therapeutic vector, which might be caused by a compensatory mechanism triggered by the overexpression of the transgene *RPS19* (Figure 4C). It is also possible that survival of potential homozygous *RPS19*-deficient cells that would not have survived otherwise was enabled by transduction with the EFS-RPS19 vector.

The edited cells showed impaired erythroid differentiation

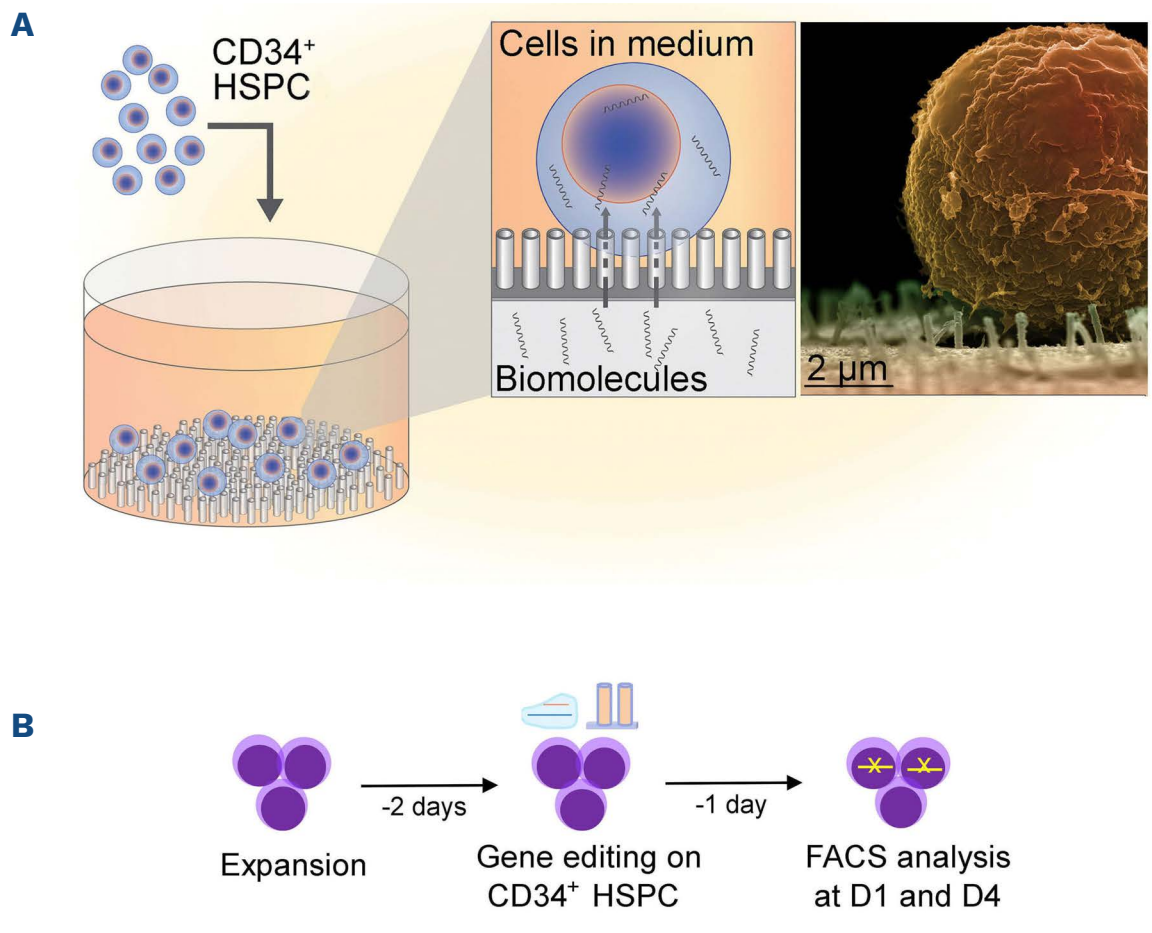

Continued on following page.

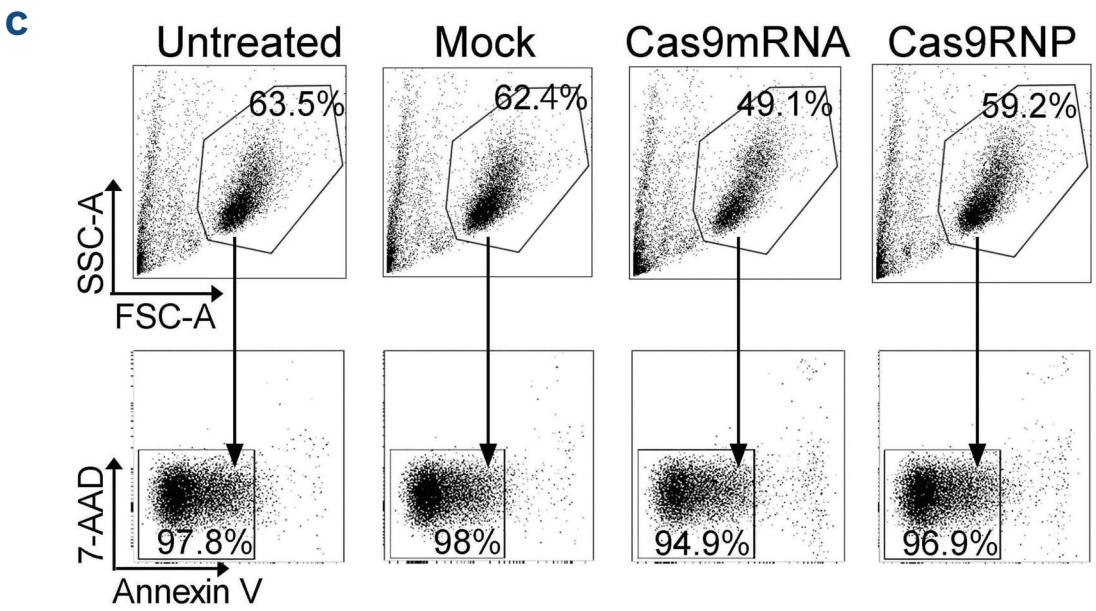

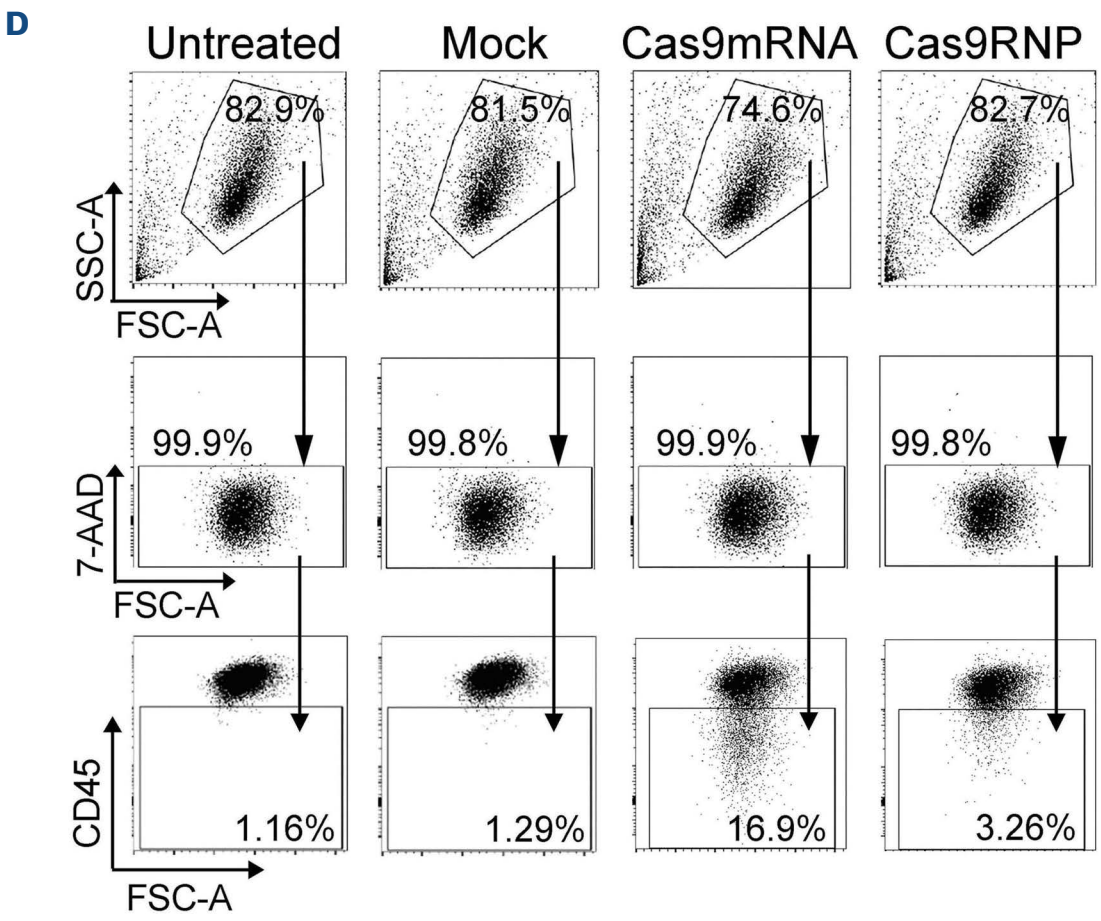

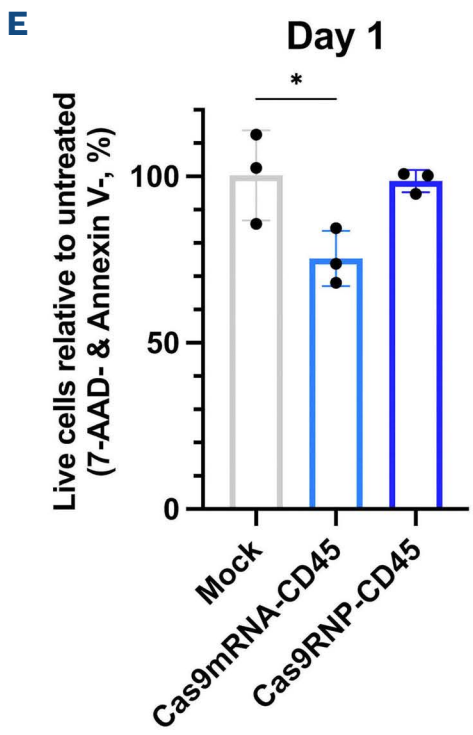

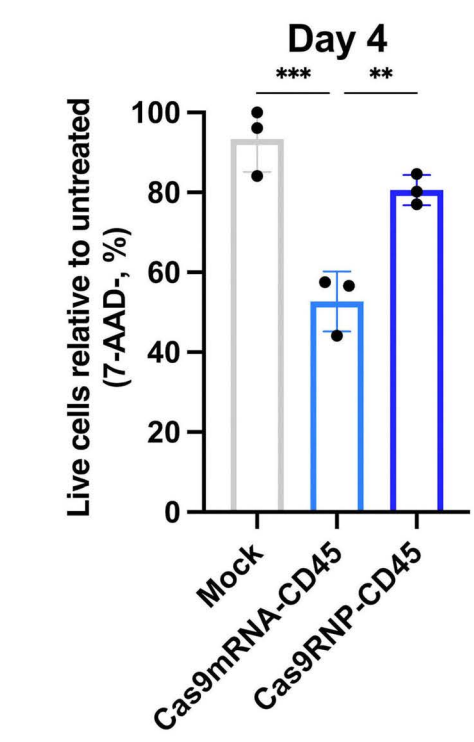

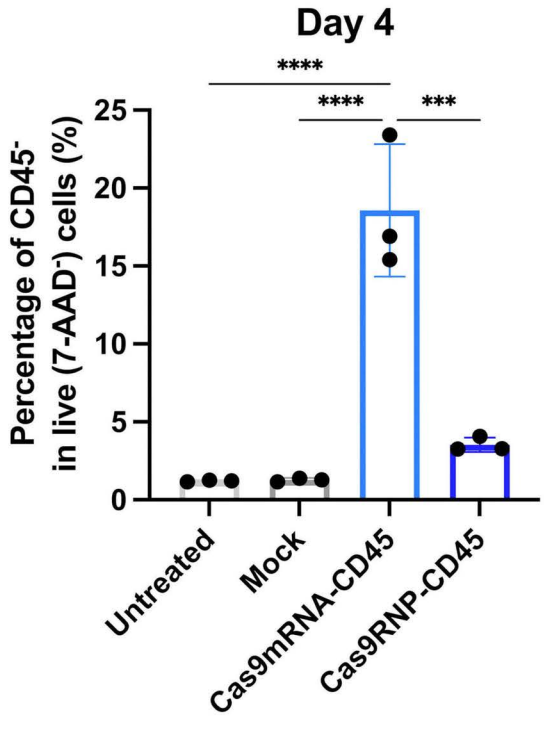

Figure 2. Nanostraw-mediated Cas9 mRNA delivery enables CD45 knockout in human hematopoietic stem and progenitor cells. (A) Schematic overview and false-colored scanning electron microscope picture of the nanostraw delivery system. (B) Timeline of experiment. (C) Representative FACS plots of cell viability (7-AAD-/Annexin-) on day 1 (D1). (D) Representative FACS plots of edited cells on day 4. (E) Percentage of live cell recovery compared to completely untreated cells on days 1 and 4 upon Cas9 mRNA and RNP delivery to knockout CD45 (*P<0.05, **P<0.01, ***P<0.001 by one-way ANOVA test, N=3). (F) Efficiency of CD45 knockout in live (7-AAD$^-$) cells on day 4 (***P<0.001, ****P<0.0001 by one-way ANOVA test, N=3). HSPC: hematopoietic stem and progenitor cells.

with increased numbers of progenitor cells ($CD71^{-}CD235^{-}$) and BFU-E/CFU-E cells ($CD71^{+}CD235^{-}$) on day 10 (Figure 4D). This is consistent with clinical observations that differentiation of patient cells is inhibited at the initial stage (BFU-E and CFU-E).[1] The erythroid differentiation block is consistently present throughout all measured timepoints (days 6, 8 and 10) during differentiation (Figure 4E). In contrast, cells treated with EFS-RPS19 could be rescued from the impaired erythroid differentiation, and showed significantly increased production of erythroblasts ($CD71^{+}CD235^{+}$) and mature red blood cells ($CD71^{-}CD235^{+}$) at all timepoints. The *RPS19*-D group produced a smaller

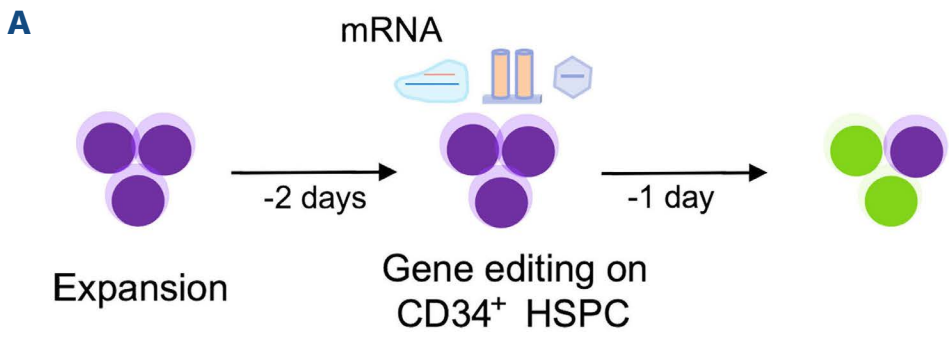

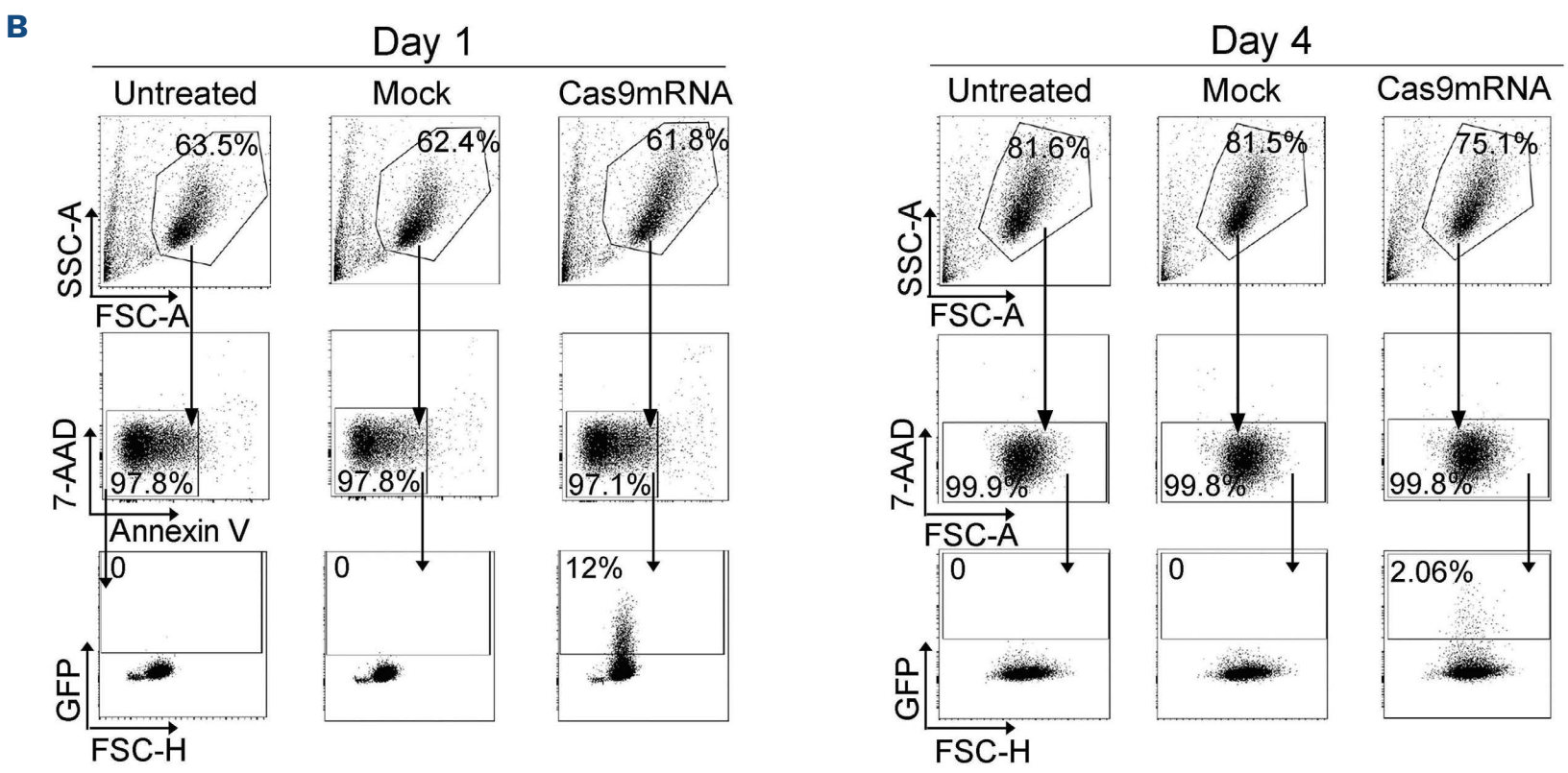

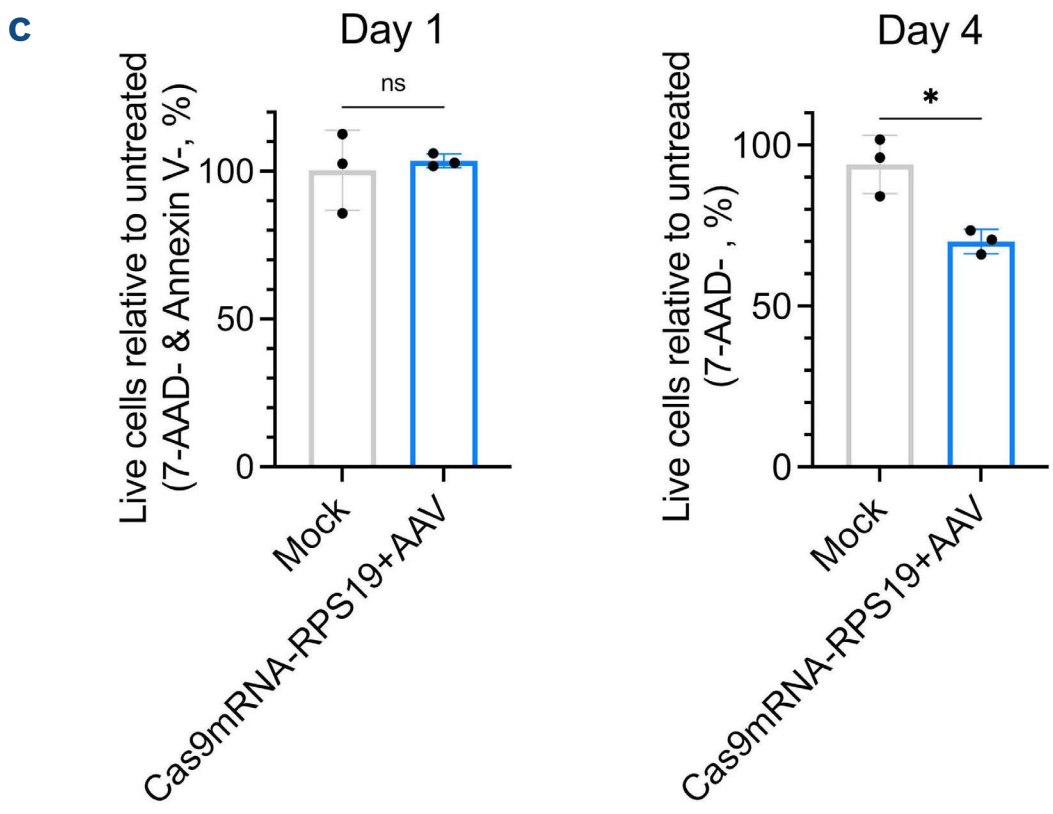

Continued on following page.

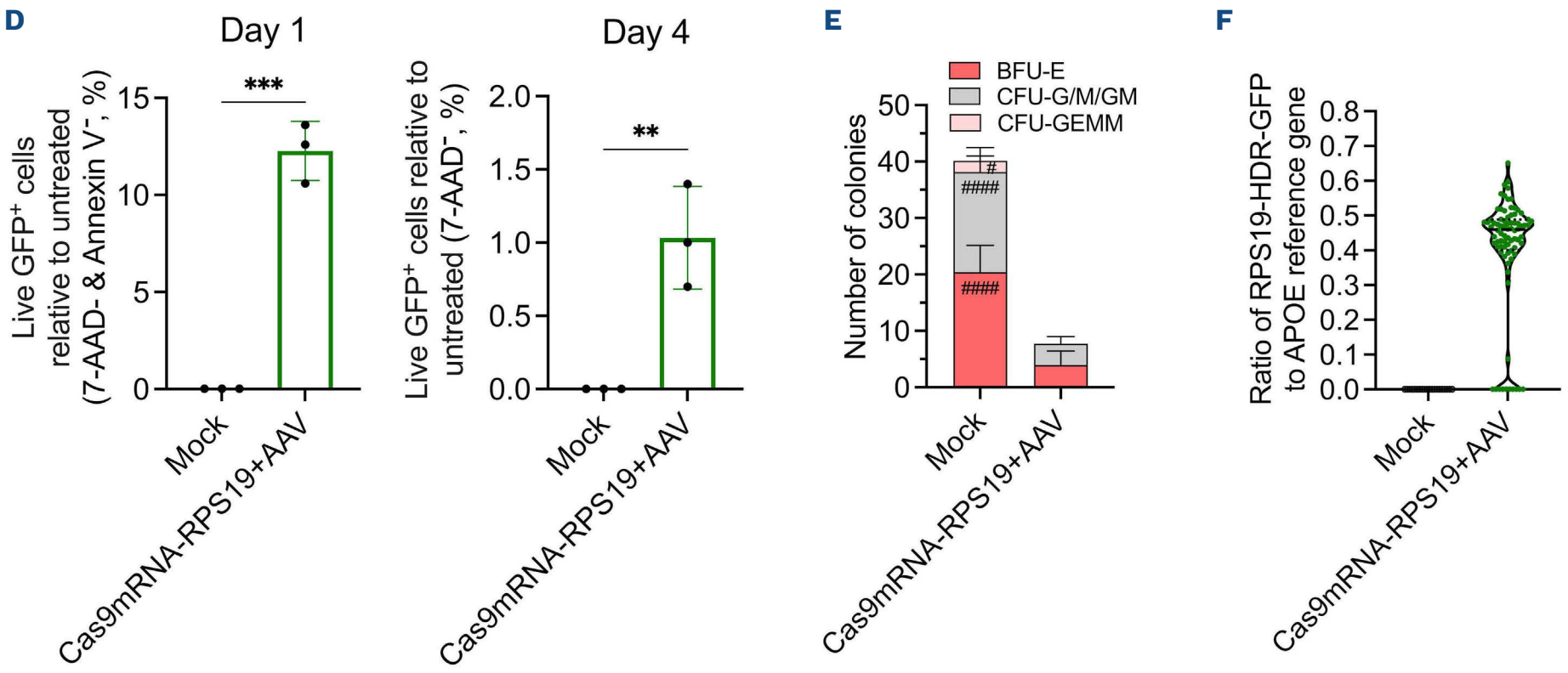

Figure 3. Delivery of Cas9 mRNA with nanostraws enables the recovery of heterozygous GFP⁺ RPS19-deficient hematopoietic stem and progenitor cells with reduced cell viability. (A) Timeline of experiment. (B) Representative FACS plots of cell viability and GFP⁺ cells on (left) day 1 and (right) day 4. (C) Percentage of live cell recovery compared to completely untreated cells on days 1 (D1) and 4 upon using nanostraw to deliver Cas9 mRNA (**P*<0.05 by *t*-test, N=3). (D) Relative percentage of GFP⁺ cells compared to total recovered live cell numbers of the untreated condition, using a nanostraw to deliver Cas9 mRNA on days 1 and 4 (***P*<0.01, ****P*<0.001 by *t*-test, N=3). (E) Number of colonies for BFU-E, CFU-G/M/GM and CFU-GEMM in each dish after culture with methylcellulose media for 14 days ($^{\#\#\#\#}P$<0.0001, $^{\#}P$<0.05 compared with the same colony category in the RPS19-deficient group by unpaired Mann-Whitney test, N=12 dishes in each group). (F) Ratio of edited allele (HDR-RPS19-GFP) to reference gene (APOE) by ddPCR (a total of 20 colonies in the mock group, and 100 colonies in the *RPS19*-deficient group were analyzed). HSPC: hematopoietic stem and progenitor cells.

and fainter red pellet compared to the CD34 group, or the Cas9-only group, while the LV-RPS19 group produced larger pellets than the *RPS19*-D group on day 21 (Figure 4F). Overall, the results show that we successfully created a RPS19-deficient model that accurately mimics the impaired DBA erythroid differentiation phenotype, which could be rescued by our therapeutic EFS-RPS19 vector.

Single-cell transcriptomic and differentiation trajectory during erythroid differentiation

We next performed single-cell RNA sequencing (scRNA-seq) to analyze the transcriptome of RPS19-D cells before and after treatment with EFS-RSP19 during the early stage of erythroid differentiation. Briefly, we cultured the sorted *RPS19*-deficient cells in erythroid differentiation medium for 6 days, followed by sorting GFP⁺ cells from the *RPS19*-D and the LV-RPS19 group, and GFP⁻negative cells from the CD34 group for scRNA-seq analysis. The expression of GFP, endogenous RPS19 and EFS-RPS19-produced RPS19 (coRPS19) were checked in each group and were consistent with our previous results (*Online Supplementary Figure S8*). Unsupervised clustering by the Leiden method identified 11 distinct clusters from all the samples.[16] We identified clusters based on the markers for hematopoietic progenitor compartments, megakaryocyte progenitors, and erythroid progenitors (EP) as described in the Methods (Figure 5A, *Online Supplementary Figure S9*). For the identified EP-related clusters, the late EPs1 (LEPs1) showed high *HBB* expression and the LEPs2 showed high *HBA1* and *HBA2* expression (Figure 5A). The expression of *GYPA* increased gradually from the LEPs1 to the LEPs3, which may indicate the gradual erythroid differentiaton. This is further supported by the gradual increased expression of *KLF1* (Figure 5A). On the contrary, both the 2 DBA EP showed lower *HBB, HBA1* and *HBA2* expression compared to the LEP. Specifically, we did not observe obvious differences on the expression of transcription factors of *GATA1* and *GATA2* among LEP clusters. In addition, cell cycle genes (*MKI67* and *AURKB*) showed very low expression in the DBA EPs1, which is also the main LEP cluster in the RPS19-D group (38.9%, Figure 5B). The DBA EPs2 showed higher *MKI67* and *AURKB* expression, but still lower expression of hemoglobin genes compared to the 3 LEP. Importantly, there was an almost 50% reduction of the DBA EPs1 cluster in the LV-RPS19 group (19.9%). Instead, the Rescued EP cluster became the main cluster (23.1%), with higher expression of hemoglobin (*HBA1, HBA2*) and cell cycle (*MKI67* and *AURKB*) genes compared to the 2 DBA EP clusters.

We next used a force-directed graph drawing algorithm, Force-Atlas2, to infer the differentiation trajectory of the cells during erythroid differentiation (Figure 5C).[17] The ob-

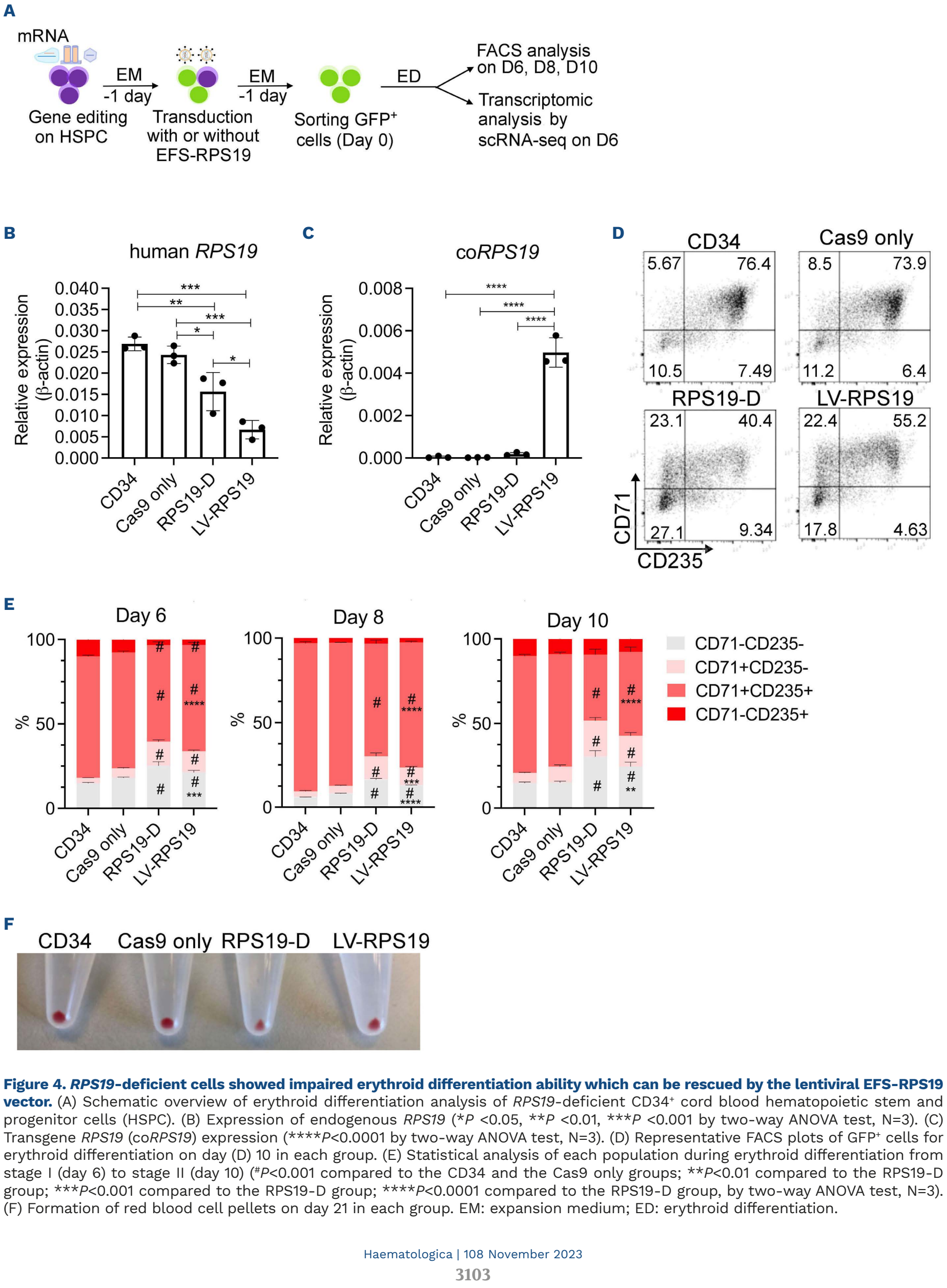

Figure 4. *RPS19*-deficient cells showed impaired erythroid differentiation ability which can be rescued by the lentiviral EFS-RPS19 vector. (A) Schematic overview of erythroid differentiation analysis of *RPS19*-deficient CD34⁺ cord blood hematopoietic stem and progenitor cells (HSPC). (B) Expression of endogenous *RPS19* (**P* <0.05, ***P* <0.01, ****P* <0.001 by two-way ANOVA test, N=3). (C) Transgene *RPS19* (co*RPS19*) expression (*****P*<0.0001 by two-way ANOVA test, N=3). (D) Representative FACS plots of GFP⁺ cells for erythroid differentiation on day (D) 10 in each group. (E) Statistical analysis of each population during erythroid differentiation from stage I (day 6) to stage II (day 10) (#*P*<0.001 compared to the CD34 and the Cas9 only groups; ***P*<0.01 compared to the RPS19-D group; ****P*<0.001 compared to the RPS19-D group; *****P*<0.0001 compared to the RPS19-D group, by two-way ANOVA test, N=3). (F) Formation of red blood cell pellets on day 21 in each group. EM: expansion medium; ED: erythroid differentiation.

tained global topology revealed high connections of the EEP with the LEP and Rescued EP, compared to the DBA EPs1, which were further supported by the partition-based approximate graph abstraction (PAGA) graph. The hemoglobin genes were highly expressed in the LEP and the Rescued EP (*Online Supplementary Figure S10*). These results indicate the abnormal erythroid differentiation of the DBA EPs1.

Overall, specific clusters were identified in the RPS19-D and the LV-RPS19 group. The Rescued EP showed reversed erythroid marker gene expressions and higher correlations with the LEP in the CD34 group than the DBA EPs1 by the differentiation trajectory analysis.

EFS-RPS19 helps to recover abnormal cell cycle in the erythroid progenitors of the RPS19-D group

Since several LEP were observed, we next focused on the their transcriptomic differences. We compared genes related to erythroid progenitors and cell cycle according to a previous publication.[3] There was an obvious reduction in the EP-related cell cycle genes in the DBA EPs1 (*TUBA1B, TUBB, TUBB4B,* etc.) (*Online Supplementary Figure S11*). On the contrary, the cell cycle-related genes were more highly expressed in the DBA Eps2, as mentioned above. We further analyzed the cell-cycle phase in all the LEP clusters. The DBA EPs1 showed a high percentage of genes in G1 phase (81.9%), while the DBA EPs2 showed a high percentage of genes in G2M (72.6%) and S phase (21.5%) compared to the other clusters (Figure 6A). Importantly, the Rescued EP showed similar cell cycle stage (G1: 54.4%; G2M: 25.9%; S: 19.7%) to the LEPs1 (G1: 55.1%; G2M: 25.9%; S: 19%). These results demonstrate the characteristics of the DBA EPs1 with impaired cell-cycle stage and lower hemoglobin gene expressions. However, treatment with the therapeutic vector could activate the cell cycle and improve hemoglobin gene expressions, as observed in the Rescued EPs. Since the cell-cycle stage in the Rescued EP reached a similar level to the LEPs 1, we applied the gene set enrichment analysis (GSEA) algorithm analysis among the LEPs1 (from the CD34 group), the DBA EPs1 (from the RPS19-D group), and the Rescued EP (from the LV-RPS19 group). TNFα, p53 and apoptosis signaling pathways were enriched in the DBA EPs1 compared to the LEPs1 and the Rescued EP (Figure 6B). On the contrary, cell cycle-related signaling pathways (e.g., MYC targets, G2M checkpoint and mitotic spindle signaling pathways)

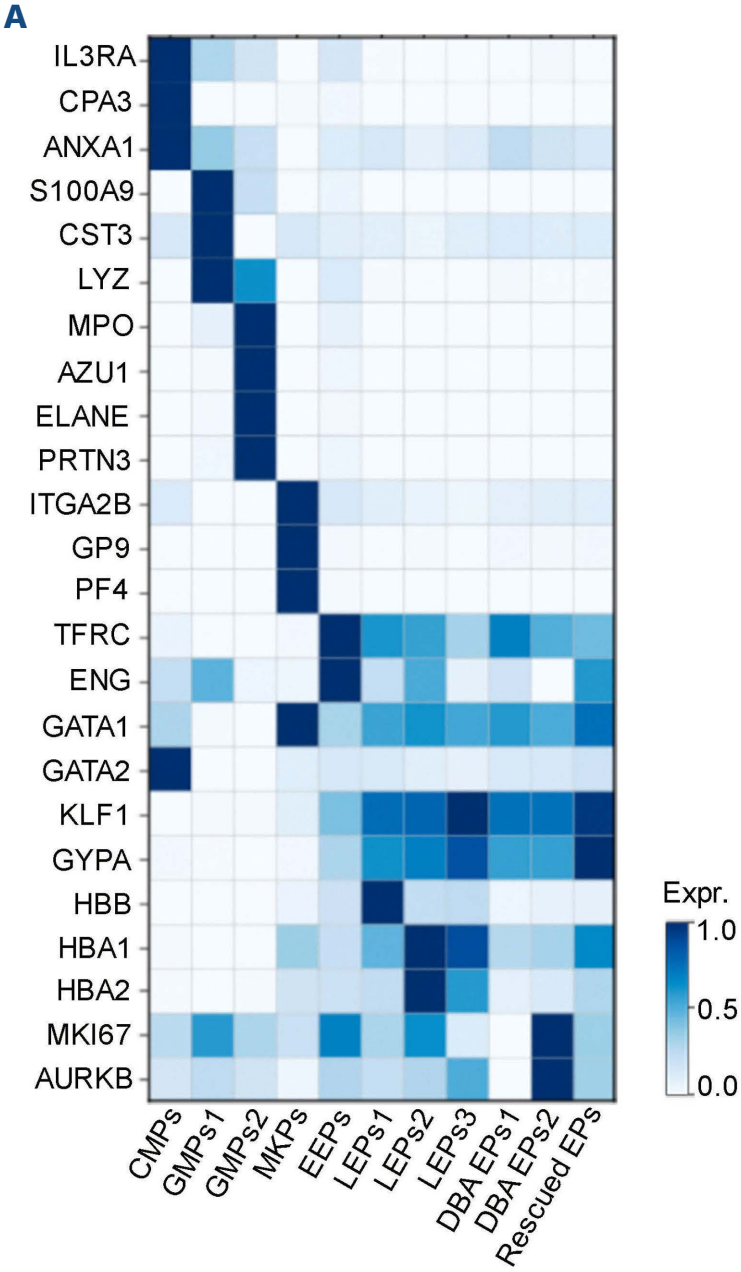

Figure 5. Clustering analysis and differentiation trajectory during erythroid differentiation. (A) Heatmap of the mean expression value of manually selected marker genes for each cluster. CMP: common myeloid progenitors; GMP: granulocyte-macrophage progenitors; MKP: megakaryocyte progenitors; EEP: early erythroid progenitors; LEP: late erythroid progenitors. (B) UMAP plot colored by (left) cluster and (middle) UMAP plot split by tissue. (Right) Frequency of each cluster in CD34, RPS19-D, and LV-RPS19 groups. (C) Partition-based approximate graph abstraction (PAGA) initialized embedding and PAGA graph of the differentiation trajectory. Size of dots is proportional to number of cells in the clusters.

Continued on following page.

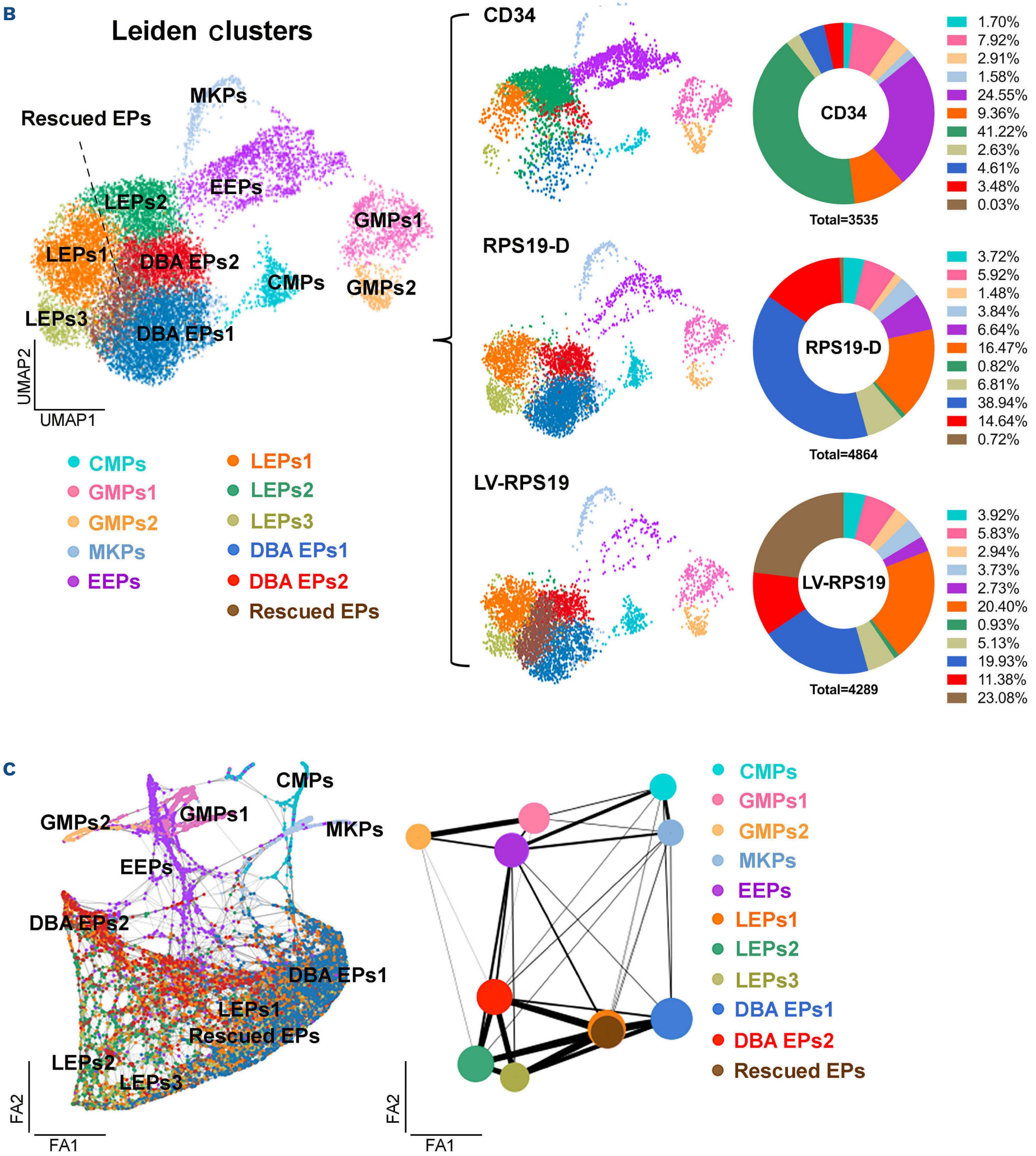

and heme metabolism were highly enriched in both the LEPs1 and the Rescued EP clusters (*Online Supplementary Tables S1, S2*). This further supports the conclusion that EFS-RPS19 could reverse the impaired erythroid differentiation of the RPS19-D cells by activating the cell-cycle status. The top 20 differentially expressed genes are shown in Figure 6C. Specifically, EFS-RPS19 could reverse the expression of several cell cycle-related genes, such as *HMGB1, HMGB2* and *TUBA1B*, which may contribute to the therapeutic effects. The recovery of the cell-cycle genes in the Rescued EP was also observed when we compared it to the LEPs2 (*Online Supplementary Figure*

S12), and some heat shock proteins (*HSP90AA1* and *HSPD1*) were also found to be highly expressed in the Rescued EP. Although the DBA EPs2 showed high expression of cell-cycle genes, low hemoglobin genes were still observed in the cluster. By comparing it with the LEP, some long non-coding RNA (lncRNA), such as *MALAT1* and *XACT*, were found highly expressed in the DBA EPs2 (*Online Supplementary Figure S13A, B*).

Taken together, we identified specific cluster with abnormal cell-cycle status and enriched TNFα, p53 and apoptosis signaling pathways in the RPS19-D group. On the contrary, the EFS-RPS19-treated cells could recover cell-cycle status through activation of cell cycle-related signaling pathways, which are similar to the levels in the CD34 group.

Discussion

Due to the very limited avaliablility of the patient samples, a traceable and precise DBA cell model would be useful to explore mechanisms and allow therapeutic investigations. We previously generated a *RPS19* knockdown cell model using shRNA.[5] However, modeling of haploinsufficient

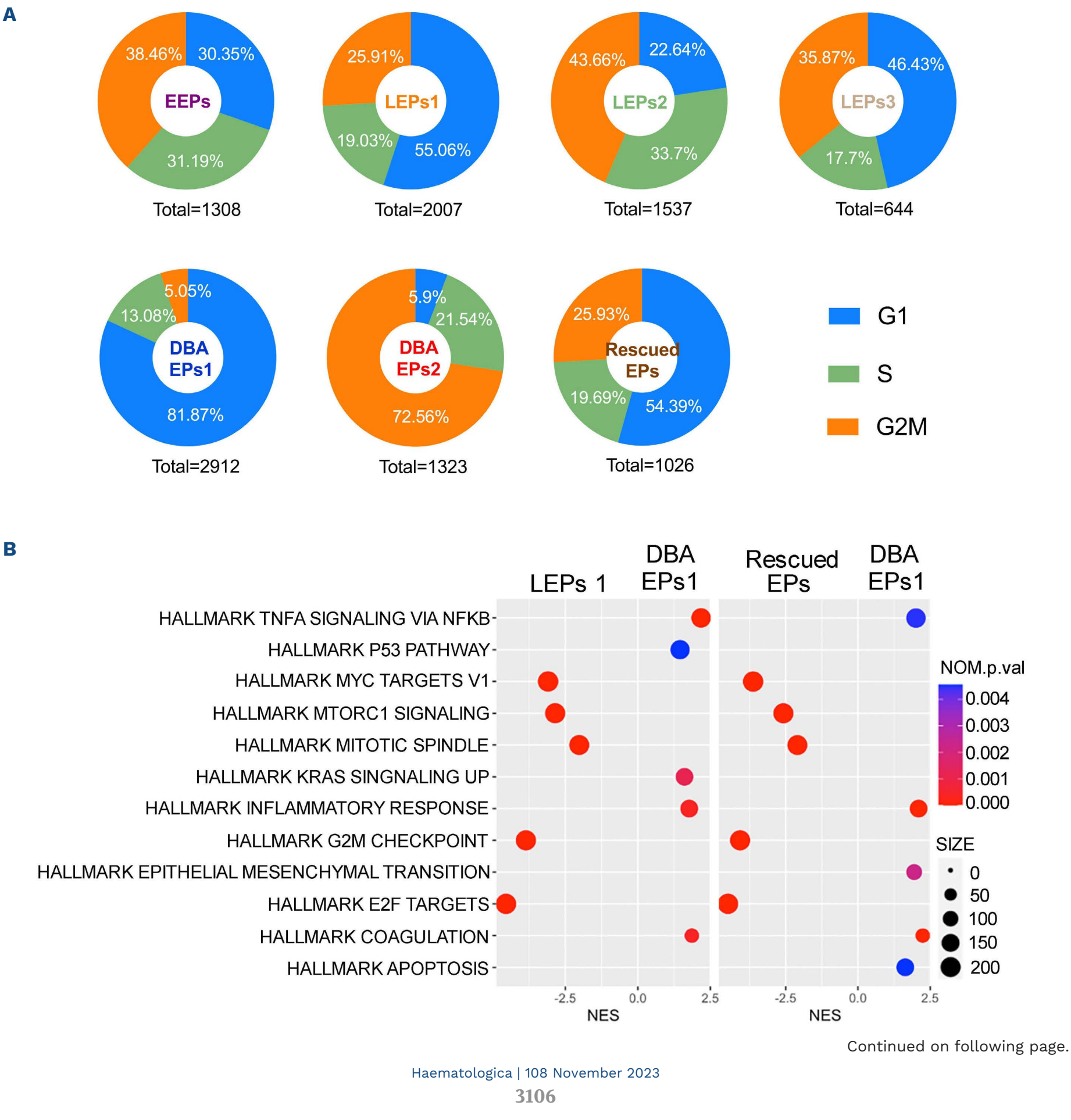

Continued on following page.

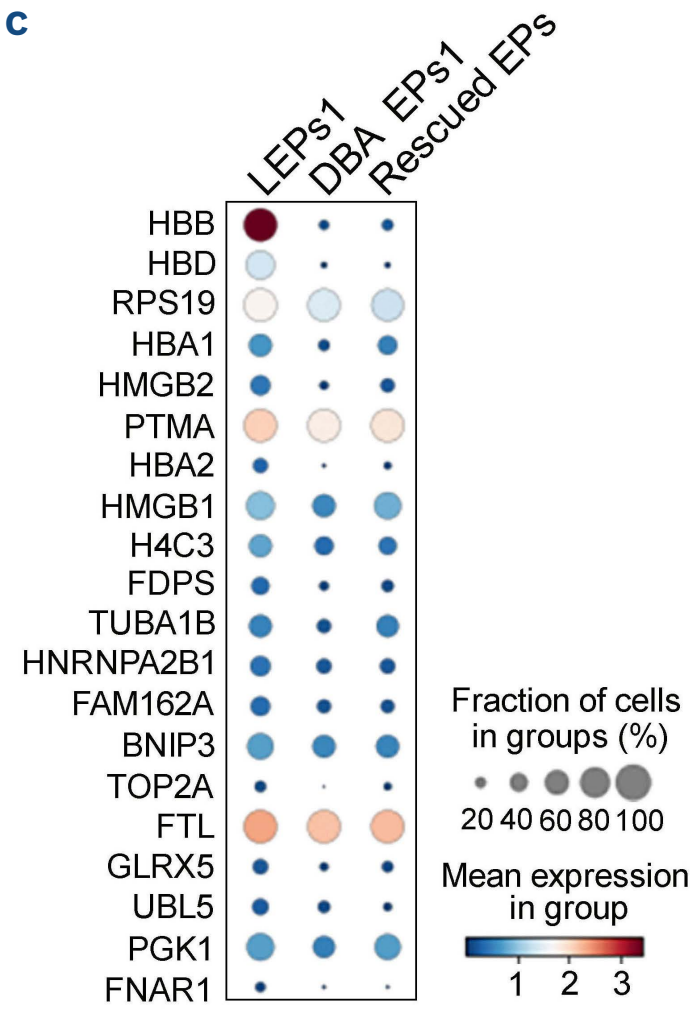

Figure 6. RPS19-deficient cells show abnormal cell cycle with activation of inflammatory signaling pathway that can be rescued by EFS-RPS19. (A) Donut plots showing percentages of cells in G1, S, and G2M phase in erythroid progenitor (EP) clusters. (B) Bubble plot showing abnormal significantly enriched signaling pathways (NOM: $P<0.05$) in the DBA EP 1 cluster from the RPS19-deficient group compared with the LEP 1 cluster from the CD34 group and Rescued EP cluster from the LV-RPS19 group. Pathways are from the Hallmark gene sets of the Molecular Signatures Database. (C) Dot plot showing the 20 top differentially expressed genes in the indicated clusters.

human diseases like DBA is challenging because the phenotype is highly dependent on the level of gene downregulation. Moreover, the shRNA-based knockdowns can be a useful approach to model the effect of disease-causing mutations, but it is difficult to precisely mimic the effect of heterozygous gene loss. Furthermore, shRNA-based knockdowns induce wide-ranging unintended off-target effects on unrelated genes. These issues make it more difficult to generate accurate disease models and to determine precise cause-effect relationships with shRNA.[18]

In this study, we set out to create a traceable *RPS19*-deficient model by using CRISPR-Cas9 to validate and generate the transcriptomic landscapes of our previously developed therapeutic lentiviral vector. Since DBA already presents early in infancy, we decided to use umbilical cord blood HSPC from healthy donors as the starting material for generating the cell model. However, working with these cells comes with multiple challenges. First, only limited numbers of cells can be obtained from each donor, which limits the scale of experiments that can be performed.[19] Second, they are highly sensitive to stress, such as that induced by electroporation.[20] Third, they are challenging to transfect.[21] In our results, the conventional method of using electroporation for Cas9 delivery turned out to be highly detrimental for the cells when *RPS19* was targeted, and did not allow sufficient recovery of edited cells. We speculate that several parts of the procedure likely contributed to the toxicity. Programmable nucleases, such as Cas9, cut DNA and induce double-stranded breaks (DSB).[22] DSB can trigger apoptosis, differentiation or replicative arrest in HSPC, and limit their long-term engraftment capacity.[9] It has also been shown that delivering Cas9 to HSPC via electroporation is toxic and activates p53, which leads to decreased cell viability and function.[14,23,24] Furthermore, electroporation itself triggers a strong stress response in HSPC, even when a more benign cargo, such as GFP mRNA, is delivered. All of this, however, is not enough to explain the extreme toxicity that we observed when targeting *RPS19* with electroporation-based Cas9 delivery, since targeting a different gene (CD45) with the same method was much less toxic and allowed for the recovery of a reasonable number of cells. Deficiencies in ribosomal genes such as RPS19 have been shown to induce the activation of p53, p21, and apoptosis.[1,25] This might have compounded the negative effects of the electroporation and DSB, and caused the complete loss of viability that we observed.

To overcome the toxicity issue, we used nanostraws to deliver Cas9 to HSPC. We adapted the nanostraws and delivery parameters to facilitate efficient disruption of *RPS19* in HSPC enabling recovery of sufficient numbers of edited cells, which make it possible to perform downstream functional studies such as verifying the therapeutic effects of our clinically-applicable lentiviral vector. This approach has allowed us to establish a geno- and phenotypically correct DBA disease model using cord blood-derived $CD34^+$ HSPC. This method of generating cell models will be useful for studying other disease-related genes that, until now, could not easily be knocked out in sensitive pri-

mary cell types.

The mechanistic basis for DBA pathophysiology is not fully understood, and this has limited the development of new therapeutic modalities. We observed a 75% recovery on the erythroid differentiation (increased CD235 expression) after treatment with EFS-RPS19. Interestingly, this is also consistent with our previously reported transduction efficiency of the vector at the same MOI.[5] By applied scRNA-seq analysis, our data indicate that the vector exerts its therapeutic effects by reversing the cell-cycle stage to promote cells to enter into cycling. Moreover, activated inflammatory signaling pathways were enriched in the *RPS19*-deficient group compared to the CD34 group and the vector-treated group. Consistent with our observation, recent studies demonstrated that elevated TNF-α can be detected in DBA bone marrow plasma,[3] and inflammatory signature was shown in erythroblasts and red blood cells from DBA patients.[26] Iskander *et al*. also demonstrated enriched TNF-α signaling via the NF-κB pathway in erythroid progenitors of DBA patients by RNA-sequencing.[3] The role of inflammatory signaling pathway is worthy of future study. On the other hand, we also identified one cluster with activated cell-cycle status, but low hemoglobin gene expression in the RPS19-D group. The underlying mechanism remains unknown; however, lncRNA such as *MALAT1* and *XACT* were found highly enriched the cluster. The *MALAT1* has been shown to be regulated by p53 and plays a significant role in maintaining the proliferation potential of early-stage hematopoietic cells.[27] This may indicate that abnormal epigenetic regulation also contributes to the impaired erythroid differentiation, which would be an interesting topic for future studies.

Overall, we successfully generated a traceable *RPS19*-deficient CD34$^+$ HSPC cell model by using nanostraws to deliver Cas9 mRNA and sgRNA. The nanostraw platform provides an optimal delivery option for targeting genes that sensitize cells to stress when knocked out, especially in sensitive primary stem cells. By using a clinically applicable lentiviral therapeutic vector EFS-RPS19, the impaired erythroid differentiation can be rescued with increased cell cycle to promote red blood cell production, which is also supported by the scRNA-seq results. Our results will encourage further investigation of the therapeutic effects of EFS-RPS19 in primary patient samples.

Disclosures

MH is a consultant for Navan Bio Inc., a startup commercializing nanostraw technology. LS, MH and JL are inventors on a patent application relating to nanostraws.

Contributions

YL, LS, MH and SK conceptualized the project and directed the research. YL, LS, MH, TDB and AR performed the experiments. YL and SL performed single cell RNA sequencing analysis. YL and LS analyzed the data. JL and AS provided materials and reagents. YL, LS, MH, JL and SK wrote the manuscript.

Acknowledgments

The authors thank Beata Lindqvist and Xiaojie Xian for lentivirus production, Jenny G Johansson for AAV production, Maria Björklund for digital droplet PCR technical assistance, and Zhi Ma for FACS technical assistance. We thank Kristijonas Žemaitis for help in characterizing colony-forming units and Veronika Žemaitė for the schematic demonstration of the nanostraw. We thank the staff in the Lund Nano Lab for assistance with tools needed for nanostraw fabrication. We thank the Center for Translational Genomics, Lund University and Clinical Genomics Lund, SciLifeLab for providing the sequencing service.

Funding

This work was supported by a Hemato-Linne grant from the Swedish Research Council Linnaeus, project grants from Swedish Research Council (to SK and MH), the Swedish Cancer Society and the Swedish Children's Cancer Society (to SK), the Tobias Prize awarded by the Royal Swedish Academy of Sciences financed by the Tobias Foundation, a clinical research grant from Lund University Hospital (to SK), European Union project grants STEMEXPAND and PERSIST, a grant from The Royal Physiographic Society of Lund, Sweden (to YL and LS), and a grant from Stiftelsen Lars Hiertas Minne (to YL).

Data-sharing statement

All data needed to evaluate the conclusions in the paper are present in the paper and/or the Online Supplementary Appendix. The scRNA-sequencing count matrix are available in the GEO database of the NCBI under the GEO accession number GSE2232.

References

1. Da Costa L, Leblanc T, Mohandas N. Diamond-Blackfan anemia. Blood. 2020;136(11):1262-1273.
2. Ulirsch JC, Verboon JM, Kazerounian S, et al. The genetic landscape of Diamond-Blackfan anemia. Am J Hum Genet. 2018;103(6):930-947.
3. Iskander D, Wang G, Heuston EF, et al. Single-cell profiling of human bone marrow progenitors reveals mechanisms of failing erythropoiesis in Diamond-Blackfan anemia. Sci Transl Med. 2021;13(610):eabf0113.
4. Khajuria RK, Munschauer M, Ulirsch JC, et al. Ribosome levels selectively regulate translation and lineage commitment in human hematopoiesis. Cell. 2018;173(1):90-103.e19.
5. Liu Y, Dahl M, Debnath S, et al. Successful gene therapy of Diamond-Blackfan anemia in a mouse model and human

CD34(+) cord blood hematopoietic stem cells using a clinically applicable lentiviral vector. Haematologica. 2022;107(2):446-456.
6. Jaako P, Flygare J, Olsson K, et al. Mice with ribosomal protein S19 deficiency develop bone marrow failure and symptoms like patients with Diamond-Blackfan anemia. Blood. 2011;118(23):6087-6096.
7. An K, Zhou JB, Xiong Y, et al. Computational studies of the structural basis of human RPS19 mutations associated with Diamond-Blackfan anemia. Front Genet. 2021;12:650897.
8. Bhoopalan SV, Yet JS, Mayuranathan T, et al. A novel RPS19-edited hematopoietic stem cell model of Diamond-Blackfan anemia for development of lentiviral vector gene therapy. Blood. 2021;138(Suppl 1):859.
9. Schiroli G, Conti A, Ferrari S, et al. Precise gene editing preserves hematopoietic stem cell function following transient p53-mediated DNA damage response. Cell Stem Cell. 2019;24(4):551-565.
10. Schmiderer L, Subramaniam A, Zemaitis K, et al. Efficient and nontoxic biomolecule delivery to primary human hematopoietic stem cells using nanostraws. Proc Natl Acad Sci U S A. 2020;117(35):21267-21273.
11. Xie X, Xu AM, Leal-Ortiz S, Cao Y, Garner CC, Melosh NA. Nanostraw-electroporation system for highly efficient intracellular delivery and transfection. ACS Nano. 2013;7(5):4351-4358.
12. Cao Y, Chen H, Qiu R, et al. Universal intracellular biomolecule delivery with precise dosage control. Sci Adv. 2018;4(10):eaat8131.
13. Chiappini C, Chen Y, Aslanoglou S, et al. Tutorial: using nanoneedles for intracellular delivery. Nat Protoc. 2021;16(10):4539-4563.
14. Bak RO, Dever DP, Porteus MH. CRISPR/Cas9 genome editing in human hematopoietic stem cells. Nat Protoc. 2018;13(2):358-376.
15. Yudovich D, Backstrom A, Schmiderer L, Zemaitis K, Subramaniam A, Larsson J. Combined lentiviral- and RNA-mediated CRISPR/Cas9 delivery for efficient and traceable gene editing in human hematopoietic stem and progenitor cells. Sci Rep. 2020;10(1):22393.
16. Traag VA, Waltman L, van Eck NJ. From Louvain to Leiden: guaranteeing well-connected communities. Sci Rep. 2019;9(1):5233.
17. Jacomy M, Venturini T, Heymann S, Bastian M. ForceAtlas2, a continuous graph layout algorithm for handy network visualization designed for the Gephi software. PLoS One. 2014;9(6):e98679.
18. Rao DD, Senzer N, Cleary MA, Nemunaitis J. Comparative assessment of siRNA and shRNA off target effects: what is slowing clinical development. Cancer Gene Ther. 2009;16(11):807-809.
19. Fares I, Chagraoui J, Gareau Y, et al. Cord blood expansion. Pyrimidoindole derivatives are agonists of human hematopoietic stem cell self-renewal. Science. 2014;345(6203):1509-1512.
20. Dever DP, Bak RO, Reinisch A, et al. CRISPR/Cas9 beta-globin gene targeting in human haematopoietic stem cells. Nature. 2016;539(7629):384-389.
21. Papapetrou EP, Zoumbos NC, Athanassiadou A. Genetic modification of hematopoietic stem cells with nonviral systems: past progress and future prospects. Gene Ther. 2005;12(Suppl 1):S118-130.
22. Kosicki M, Tomberg K, Bradley A. Repair of double-strand breaks induced by CRISPR-Cas9 leads to large deletions and complex rearrangements. Nat Biotechnol. 2018;36(8):765-771.
23. Haapaniemi E, Botla S, Persson J, Schmierer B, Taipale J. CRISPR-Cas9 genome editing induces a p53-mediated DNA damage response. Nat Med. 2018;24(7):927-930.
24. Enache OM, Rendo V, Abdusamad M, et al. Cas9 activates the p53 pathway and selects for p53-inactivating mutations. Nat Genet. 2020;52(7):662-668.
25. Vlachos A, Ball S, Dahl N, et al. Diagnosing and treating Diamond Blackfan anaemia: results of an international clinical consensus conference. Br J Haematol. 2008;142(6):859-876.
26. Kapralova K, Jahoda O, Koralkova P, et al. Oxidative DNA damage, inflammatory signature, and altered erythrocytes properties in Diamond-Blackfan anemia. Int J Mol Sci. 2020;21(24):9652.
27. Ma XY, Wang JH, Wang JL, Ma CX, Wang XC, Liu FS. Malat1 as an evolutionarily conserved lncRNA, plays a positive role in regulating proliferation and maintaining undifferentiated status of early-stage hematopoietic cells. BMC Genomics. 2015;16(1):676.